

Effects of the ketogenic diet in mice with hind limb ischemia

Adilan Shalamu (✉ Adeeleh@163.com)

Fudan University

Zhen Dong

National Health Commission

Bowen Liu

Fudan University

Lihong Pan

National Health Commission

Yun Cai

Fudan University

Liwei Liu

Fudan University

Xiurui Ma

Shan Xi Cardiovascular Hospital

Kai Hu

Fudan University

Aijun Sun

Fudan University

Junbo Ge

Fudan University

Research Article

Keywords: ketogenic diet, hind limb ischemia, blood perfusion, tissue recovery

Posted Date: June 29th, 2022

DOI: <https://doi.org/10.21203/rs.3.rs-1645846/v2>

License: © ⓘ This work is licensed under a Creative Commons Attribution 4.0 International License.

[Read Full License](#)

Abstract

Background: The ketogenic diet (KD) has anti-tumor and anti-diabetic effects in addition to its anti-epileptic role. It could also improve cardiac function and attenuate neurological insult. However, the effect of the KD on blood flow or tissue recovery after ischemia remains largely unknown. Thus, we observed blood flow and ischemic tissue recovery following hind limb ischemia in mice.

Methods: C57 mice were fed with either a KD or normal diet (ND) for 2 weeks, before inducing hind limb ischemia, blood perfusion of ischemic limb tissue was observed at 0, 7, and 21 days post operation.

Results: KD not only decreased blood perfusion of ischemic limb tissue but also delayed muscle recovery after ischemia, induced muscle atrophy of non-ischemic tissue compared to mice fed with ND. Furthermore, KD delayed wound healing at the surgical site and aggravated inflammation of the ischemic tissue. At the cellular level, KD altered the metabolic status of limb tissue by decreasing glucose and ketone body utilization while increasing fatty acid oxidation. Following ischemia, glycolysis, ketolysis, and fatty acid utilization in limb tissue were all further reduced by KD, while ketogenesis was mildly increased post KD in this mice model.

Conclusion: The KD may cause impaired tissue recovery after ischemia and possible muscle atrophy under a prolonged diet. Our results hint that patients with limb ischemia should avoid ketogenic diet.

Introduction

The ketogenic diet (KD) is a low-carbohydrate diet that is high in fat and strictly limits the intake of sugars, which is recognized as an effective anti-epileptic treatment. In 1911, Gulep and Marie recorded starvation as a treatment for epilepsy; in 1921, Dr. Geyelin, an endocrinologist at New York Presbyterian Hospital, reported his experience with fasting as a treatment for epilepsy at the [1]. After studying metabolic changes under starvation later in 1921, Woody-Att noted that acetone and beta-hydroxybutyric acid appear in normal subjects through starvation or a diet containing too low a proportion of carbohydrate and too high a proportion of fat; therefore, what was termed a “ketogenic diet” was widely used throughout the 1920s and the 1930s [1,2]. Along with the discovery of new medicines for epilepsy, KD then became a last treatment option for epilepsy. In addition, KD became widely used as a treatment for obesity in the 1970s.

Ketone bodies, are short-chain fatty acids produced during the β -oxidation of fatty acids in the liver and delivered to extrahepatic tissues for energy supply by blood circulation. When the body encounters starvation or extreme exercise, the liver starts to produce ketone bodies, thereby increasing the uptake and usage of ketones by extrahepatic tissues (especially the brain, heart, and skeletal muscles) for energy supply [3]. Aside from the starvation state, hyperketonemia has also been found in diabetes, pregnancy, neonatal period, and adherence to low carbohydrate diets [4]. Circulating total ketone body concentrations in healthy adult humans are usually within 100 to 250 μ M, and rise to \sim 1 mM after

prolonged exercise or 24 h of fasting, and can be as high as 20 mM in pathological states such as diabetic ketoacidosis [5, 6].

A new perspective on KD has recently emerged due to observed anti-cancer and anti-diabetic effects. Numerous studies have reported improvement of diabetes by lowering body weight and blood glucose, and by improving insulin resistance. KD has also been reported to provide an insulin secretagogue effect by improving islet cell function [7]. Most studies have reported that KD inhibits the growth of tumors in pancreatic cancer, glioblastoma, and brain cancer [8-10]. Identifying the signaling effects of ketone bodies has introduced a broad trend of further investigation reporting that KD presents a significant neuroprotective and possibly therapeutic effect in non-alcoholic fatty liver disease [11, 12]. In addition, significant improvement of cardiac function in patients with heart failure has drawn attention, suggesting that KD may have therapeutic value in heart failure treatment by increasing blood ketone levels; this finding was further supported by the presence of SGLT2 inhibitors [13-15].

Angiogenesis is fundamental to many physiological and pathological processes such as ischemia and inflammation. Myocardial and limb ischemia are common diabetic complications caused by a diseased metabolic environment as hyperglycemia, hyperlipidemia and hyperketonemia. Fasting and calorie restriction also increase blood ketone levels and alter body metabolism similarly to KD by changing the expression of FOXO- and PGC-1-related genes [16]. Calorie-restricted diets reduce angiogenesis, whereas fasting induces angiogenesis by improving endothelial progenitor cells in mice [17-20]. Moreover, a lack of ketolysis-related enzymes was found to significantly impair lymph vessel growth in mice [21]. However, how ketone bodies effect blood vessel growth during angiogenesis, and how they affect blood perfusion under ischemic conditions remains unknown. Therefore, we conducted this study to fully observe blood flow and ischemic tissue recovery following hind limb ischemia in mice fed a KD. We found that KD not only reduced blood perfusion in ischemic tissue but also induced muscle atrophy and ischemic tissue fibrosis along with delayed wound healing in mice.

Materials And Methods

2.1 Animals and diet

C57BL/6N mice aged 8–10 weeks (weight 22–25 g) were purchased from Gem Pharma Tech LLC (Nanjing, Jiangsu, China) and maintained in a 12/12-h light/dark cycle environment at a constant temperature of 22°C with free access to standard laboratory chow and tap water. Mice were divided into normal diet (ND) group and ketogenic diet (KD) group (n=13 in each group) fed with standard chow and ketogenic chow respectively (Table 1 purchased from Xietong Pharma Co., Jiangsu, China), with free access to food and water 24hs. After 2 weeks, mice underwent hindlimb ischemia by ligation of the unilateral femoral artery and were given continued access to the two different diets. After the procedure, mice were evaluated for ischemic hindlimb blood perfusion using a laser Doppler perfusion imager. All animal experimental procedures conformed to the Guide for the Care and Use of Laboratory Animals

published by the US National Institutes of Health (NIH publication no. 85–23, revised 1996) and were reviewed and approved by the Animal Ethics Committee at Zhongshan Hospital, Fudan University, China.

2.2 Measurement of plasma metabolic parameters

Blood glucose and ketone levels (represented by β -hydroxybutyrate levels) were measured using a glucose meter and ketone meter, respectively (Abbott Diabetes Care, Maidenhead, UK). Tissue β -HB content was measured by β -Hydroxybutyrate (β -HB) assay kits (MAK041, Sigma, Kawasaki, Kanagawa). Tissues were homogenized in cold β -hydroxybutyrate assay buffer and centrifuged at 13,000 g for 10 min at 4°C to remove insoluble material.

2.3 Hind-limb ischemia procedure

To establish a hind limb ischemia (HLI) model, we performed unilateral femoral artery ligation in mice. Following percutaneous injection of the anesthetic (4% chloral hydrate), a groin incision was made in the left adductor hind-limb region. The femoral artery was identified, ligated with 6–0 silk ties at the ends of the vascular trunk, and transected from the middle. The incision was then closed with interrupted non-absorbable sutures, and mice were closely monitored for 24 h post-procedure.

2.4 Doppler perfusion

Mice were subjected to an inhaled anesthetic at body temperature maintained by a warming pad. A laser Doppler perfusion imager (Periscan PIM3, Perimed, Beijing, China), was used to evaluate the bilateral hindlimbs. Perfusion was evaluated in the whole limb, gastrocnemius region, and hind-paw region on post-HLI days 0, 7, and 21.

2.5 Staining

Gastrocnemius muscle tissues were fixed in 4% paraformaldehyde, dehydrated, and embedded in paraffin then dehydrated in graded ethanol solutions and toluene. Tissues were dissected into 5- μ m-thick sections and stained with hematoxylin and eosin (H&E) and Masson. For immunofluorescence staining, the sections were blocked with 10% goat serum albumin (Invitrogen, Waltham, Massachusetts, USA) for 60 min before staining with CD31 monoclonal antibody (1:1500, CST).

2.6 Immunoblotting

Total protein was extracted from the gastrocnemius tissue. Equal amounts of protein extract were separated by SDS-PAGE and transferred to polyvinylidene difluoride membranes. The membranes were blocked with 5% bovine serum albumin and probed with primary antibodies individually at 4°C overnight. After subsequent washing, the blots were incubated with horseradish peroxidase-coupled anti-rabbit or anti-mouse secondary antibodies at room temperature for 2 h. The blots were visualized and detected by chemiluminescence reaction (Luminata™ Forte, Millipore, Burlington, Massachusetts, USA) and ChemiDoc™ Imaging System (Bio-Rad, Hercules, CA, US). The density of the protein blots was determined

using ImageJ software (1.50i, Open Source, USA) and normalized to β -actin (1:1000, Kang Chen, Wuxi, China).

2.7 RNA procedures

Total RNA from gastrocnemius tissues was extracted using TRIzol™ Reagent (#15,596,026, Invitrogen, Waltham, Massachusetts USA). The concentration and purity of RNA were determined by Nanodrop (Thermo Fischer, Waltham, Massachusetts, USA), and 1000 ng RNA was purified with an A260/A280 ratio of 1.8–2.0 and then reverse transcribed into cDNA using PrimeScript™ Reverse Transcription Master mix (# RR036A, TaKaRa, Kusatsu, Shiga, Japan). Reverse transcription polymerase chain reaction (RT-PCR) was performed using PrimeScript™ RT Master Mix (TaKaRa, Japan). A total of 20 μ L reaction system was used, including DNA template 1.6 μ L and SYBR 10 μ L, and primers 0.4 μ L and ddH₂O 7.6 μ L. Primers used in this study are listed in Table 2. The PCR reaction cycles were set as follows: 30 s at 95°C, then 5 s at 95°C and 30 s at 60°C for 40 cycles. Fluorescence signals were normalized to Actb using the $2^{-\Delta\Delta CT}$ method.

2.8 Statistical analysis

All statistical analyses were performed using Prism 7.0 (GraphPad Software, Inc., La Jolla, CA, USA). Continuous variables are expressed as mean \pm standard error of the mean (SEM). Normal distribution was determined using the Shapiro–Wilk test. Differences in normal variates were tested using the Student's t-test (within two groups) or a one-way analysis of variance (ANOVA, among three groups or more), with post hoc comparisons using the Tukey's multiple comparisons test. Non-normal data were analyzed using the Mann–Whitney U test or the Kruskal–Wallis H test. Statistical significance was defined as two-tailed $P < 0.05$ (*), $P < 0.01$ (**), and $P < 0.001$ (***)

Results

1. Ketogenic diet induced weight loss and affected metabolite levels in blood and tissues

After feeding for 2 weeks, we measured the body weights, and found it to be significantly lower in the KD group than in the ND group (Fig. 1A). We also measured random blood glucose and blood ketone levels (represented by blood β -hydroxybutyrate) using glucose and ketone meters during 4 weeks of feeding. We did not find a significant change in random blood glucose levels in ND-fed mice; in KD-fed mice, however, blood glucose gradually decreased in the first 2 weeks then remained stable in the third and fourth weeks (Fig. 1B). Similarly, there was no significant change in blood ketone levels of ND-fed mice; conversely, in mice fed the KD, there was a remarkable increase in blood ketone levels in the first week of feeding, reaching 2.7 mmol/L, then gradually returning to approximately 2 mmol/L in the second week and mostly remaining stable in third and fourth weeks (Fig. 1C). Finally, we measured β -hydroxybutyrate content in different tissues including the muscle, heart, and liver using a β -hydroxybutyrate assay kit, and found that β -hydroxybutyrate levels increased in the heart and muscle tissues of mice in the KD group, with a greater

increase in the heart tissue compared with mice in the ND group. There was no significant difference in β -hydroxybutyrate content in liver tissues between the two groups (Fig. 1D).

2. KD impaired perfusion recovery and revascularization in chronic hind limb ischemia

To examine the effect of KD on perfusion recovery ability in chronic ischemic injury, a mouse ischemic limb model was used in mice fed both the KD and ND. Perfusion was assayed by laser Doppler perfusion imaging on days 0, 7, and 21 following femoral artery ligation surgery. We observed that the KD reduced perfusion signals associated with more pronounced non-perfusion signals in ischemic limbs than in mice fed the ND on days 7 and 21 (Figure 2A). Quantitatively, we calculated the ratio of perfusion between ischemic and non-ischemic limbs for each mouse and found that the perfusion ratio was 86.2% at the 3-week point in the ND group, whereas it was only 52.4% in the KD group. There were no significant differences between the two groups on day 0, indicating slow recovery of limb circulation caused by KD (Figure 2B). To assess the angiogenic effect, capillary density was measured. Using immunofluorescence staining, capillary density was detected using anti-CD31 antibody in the hindlimb (Figure 2C). The micrographs showed that ischemic limbs of KD-fed mice displayed reduced capillary density (less red CD31 (+) signal), indicating reduced angiogenesis (Figure 2D). This was confirmed by western blot (WB) and quantitative PCR (qPCR) results of CD31 and vascular endothelial growth factor A (VEGFA), two common indicators of tissue revascularization [22]. By performing qPCR, we found that the mRNA levels of both CD31 (platelet endothelial cell adhesion molecule-1) and VEGFA were significantly reduced in the ischemic hind limb tissue of mice in the KD group compared with those in the ND group (Figure 2E). Further WB tests showed that both CD31 and VEGFA protein expression levels significantly decreased in the hind limb tissues of KD mice following ischemic surgery compared with mice in the ND group, but no significant difference was found in limb tissues between the KD and ND groups before ischemic surgery, indicating that KD reduced revascularization in hind limb tissue after ischemia (Figure 2F). Overall, these data indicate that KD impeded revascularization and blood perfusion of hind limb tissue after ischemia.

3. KD induced muscle atrophy

To assess the effect of KD on muscle regeneration and recovery following hind limb ischemia, we observed gastrocnemius muscle shape and weighed gastrocnemius muscle mass of both legs of mice fed KD and ND 28 days after surgery. We observed obvious atrophy of the gastrocnemius muscle on both legs of KD mice compared with those of mice in the ND group (Fig. 3A). To further confirm muscle atrophy in KD mice, we then assessed gastrocnemius muscle mass and found that the net weight of both the ischemic and lateral gastrocnemius muscles of mice in the KD group significantly decreased compared with that of mice in the ND group, indicating that KD not only induced muscle atrophy of the ischemic limb but also caused atrophy in non-ischemic muscle (Fig. 3B). We analyzed the muscle recovery rate by calculating the ratio of ischemic gastrocnemius muscle weight to lateral gastrocnemius muscle weight of each mouse and found that the recovery ability of the gastrocnemius muscle after ischemia was reduced in KD mice compared with mice in the ND group (Fig. 3C). We further assessed the

effect of KD on muscle regeneration ability by H&E staining of the gastrocnemius muscle of the ischemic hind limb. We observed irregular and small muscle fibers in the KD group compared to the ND group (Fig. 3D) and found that the calculated regenerating area decreased in mice fed KD based on H&E staining (Fig. 3E). Since we found muscle atrophy both in ischemic and nonischemic limb tissues, we hypothesized that there may be other causes for muscle atrophy besides reduced blood flow, thus we further examined whether muscle atrophy-related genes (FOXO3 and LC3)[23] were involved in this process. We found mRNA expression levels of both FOXO3 and LC3 genes were significantly decreased in ischemic hind limb tissues of mice in the KD group compared with mice in the ND group (Fig. 3F), indicating that induction of muscle atrophy-related gene expression may be one of the reasons for muscle atrophy caused by KD.

4. KD delayed wound healing and increased toe necrosis rate

We observed wound healing at the surgical site in each mouse and found that surgical wounds of mice in the ND group healed much faster than those of mice in the KD group. Images of wound closure in mice 28 days after hind limb surgery showed that the surgical wound of each mouse in the ND group healed completely when inflammatory and purulent exudation was observed at the surgical wound of mice in the KD group, indicating that KD significantly delayed wound healing and caused inflammation around the surgical sites (Fig. 4A). We also observed severe toe necrosis in KD mice and analyzed the necrosis ratio of toes in the two groups using necrosis score (1 point for toenail blackening, 3 points for toe necrosis, and 5 points for foot having fallen off) and found a higher ratio of toe necrosis in the KD group than in the ND group (Fig. 4B). H&E staining also revealed massive inflammatory cell infiltration in ischemic hind limb tissue in the KD group, while there was no sign of inflammation in the ND group (Fig. 4C). The ratio of necrotic area analysis based on H&E staining showed a significantly higher ratio of necrotic area in the KD group than in the ND group (Fig. 4D). According to a previous study, KD has anti-inflammatory effects by reducing the inflammasome (NLRP3) and inflammatory gene expression, such as IL- β and IL-6 [24]. Therefore, we further examined the expression of inflammation-related genes (IL- β , IL-6, and IL-18) in the ischemic hind limb tissue of mice in the ND and KD groups and found that KD significantly decreased inflammatory gene expression in ischemic limb tissues, further explaining the aggravated inflammation in KD mice (Fig. 4E).

5. KD induced ischemic limb tissue fibrosis

We evaluated the effect of KD on limb tissue fibrosis after ischemia using Masson staining and examination of fibrosis-related gene expression. Masson staining images showed severe fibrosis in the ischemic hind limb tissue of mice in the KD group compared to that of mice in the ND group (Fig. 5A). Additionally, analysis of the fibrotic area in the two groups based on Masson staining showed a significant increase in the fibrotic area of ischemic hind limb tissue of mice in the KD group compared with that of those in the ND group (Fig. 5B). We then examined the gene expression levels of Cola2 and α -SMA to further evaluate fibrosis, and found that both Cola2 and α -SMA mRNA expression levels

increased in the ischemic limb tissue of mice in the KD group compared with those in the ND group (Fig. 5C). Moreover, this was consistent with the finding of increased α -SMA protein expression in ischemic tissue of mice in the KD group (Fig. 5D). We also found α -SMA protein expression was slightly increased in non-ischemic tissue of mice in the KD group compared to that of mice in the ND group, indicating that KD can also trigger fibrosis without an ischemic condition.

6. KD affected hind limb tissue metabolism both before and after ischemia at the genetic level

To understand the cellular impact of the KD, we investigated the metabolic status of hind limb tissues by examining metabolism-related genes, including those present during glycolysis (represented by GLUT4, GLUT1, HK2, and PDK1), fatty acid oxidation (represented by CD36 and CPT1), and ketone body metabolism (represented by HMGCS2, BDH1, and SCOT), before and after ischemic surgery. qPCR analysis of hind limb tissues before ischemia in the two groups of mice showed that KD significantly decreased glycolysis by decreasing GLUT4, GLUT1, and HK2 gene expression and increasing PDK1 gene expression (Fig. 6A), while it increased fatty acid utilization by increasing CD36 and CPT1 gene expression compared with ND mice (Fig. 6B). Ketolysis was simultaneously reduced by decreased BDH1 and SCOT gene expression in KD mice, while there was no significant difference in ketogenesis between the two groups represented by HMGCS2 gene expression (Fig. 6C). qPCR performed subsequently in ischemic limb tissues of mice in the two groups on day 7 after ischemic surgery showed that KD further decreased glycolysis in limb tissue after ischemia (Fig. 6D). In contrast to the result of increased fatty acid oxidation found in non-ischemic tissue of mice fed with KD (Fig. 6E), fatty acid oxidation was decreased in limb tissue after ischemia. The effect of KD on ketone metabolism in ischemic tissue was observed by further decreased ketolysis and increased ketogenesis, which also differed from the results observed in non-ischemic tissue (Fig. 6F).

7. KD affected hind limb tissue metabolism both before and after ischemia at the protein level

We further evaluated the metabolic changes caused by KD at the protein level in the hind limb tissues before and after ischemia. We performed WB (Fig. 7A) and found that KD decreased glucose uptake in the hind limb tissue of mice both before and after ischemia, as represented by GLUT4 and GLUT1, while a decrease was more significant in ischemic tissue (Fig. 7B, C). We further investigated how KD affects glycolysis, and found that expression of the HK2 protein, a glycolytic enzyme, was also decreased in the hind limb tissue of KD mice both before and after ischemia, but with a more significant decrease in ischemic tissue than that in mice in the ND group (Fig. 7D). However, PDK1 protein, an inhibitor of glycolysis, showed increased expression in hind limb tissue both before and after ischemia in KD mice, with a greater increase in ischemic tissue than that in mice in the ND group (Fig. 7E). The above results indicated that KD decreased glycolysis in hind limb tissue at the protein level, both before and after ischemia, and that it produced a greater decrease after ischemia. We examined CPT1 protein expression, representing fatty acid uptake, and found that it was increased in hind limb tissue of KD mice before ischemia, but decreased after ischemia compared with ND mice, indicating that KD increased fatty acid

utilization of limb tissue before ischemia, and decreased its utilization under ischemic conditions (Fig. 7F). We also observed BDH1 and SCOT protein expression level, representing ketolysis of limb tissue; these were decreased in limb tissue of mice both before and after surgery in the KD group, while the decrease was more significant in limb tissue after ischemia compared to that of mice in the ND group (Fig. 7G, H).

Discussion

We conducted this experiment to observe how KD affects blood perfusion and tissue recovery after hind limb ischemia in mice. We found that KD impaired angiogenesis and blood recovery of hind limb tissue after ischemia in mice, induced muscle atrophy, and delayed wound healing. We found aggravated inflammation and accelerated fibrosis of ischemic limb tissue underneath in mice fed with KD. These findings indicate that KD impairs the recovery process of tissues which underwent ischemia, and increases the risk of delayed tissue recovery after ischemia under a KD. It may also partially explain the reduced angiogenesis found in ischemic tissues, in an uncontrolled diabetic state with ketosis, and also highlights the possibility that muscle atrophy develops under a KD.

We found a significant decrease in the body weight of mice after 2 weeks of KD feeding. Although several studies reported body weight loss by KD in both humans and animals, Kozue et al. and Evan et al. reported that prolonged KD did not affect body weight in mice [25, 26], indicating that KD causes a rapid drop in body weight, but that it gradually returns to the initial level, and may even increase afterwards. While the effect of KD on blood ketone levels is established, its effect on blood glucose level remains controversial. Interestingly, we found that ketone content in the liver of KD mice was not significantly different from that in mice in the ND group; however, ketone levels of muscle and heart tissue in KD mice were higher than those in ND mice, indicating that increased ketogenesis in the heart and muscle tissues of KD mice may contribute to the increased blood ketone levels in ways other than ketogenesis in the liver. The random blood glucose levels of KD mice gradually decreased in the first 2 weeks of feeding, and remained stable thereafter. This was consistent with a report of decreased blood glucose levels caused by a calorie-restricted diet due to its effect on glucose-insulin homeostasis [27].

Most importantly, we found that KD impaired angiogenesis and blood recovery after hind limb ischemia in mice, consistent with the finding of decreased angiogenesis in tumors by a calorie-restricted diet [18, 19]. The indispensable contribution of ketone metabolism to lymph vessel formation *in vivo*, indicates that ketones are not merely a metabolite [21]. In our study, KD not only reduced blood perfusion in the ischemic hind limb but also decreased CD31+ number and downregulated CD31 and VEGFA expression, indicating reduced angiogenesis in ischemic limb tissue caused by KD. Due to reduced CD31 and VEGFA expression in ischemic limb tissue of KD mice, we hypothesized that endothelial cells may play a major role in reducing angiogenesis; however, this requires further study.

We observed muscle atrophy caused by KD by visual inspection of muscle shape and mass, along with microscopic observations; our findings matched the results of a study that also reported that KD induced

muscle atrophy in mice [28]. Muscle atrophy in the KD group was also detected in non-ischemic limb muscles, indicating that there may be causes of muscle atrophy other than reduced blood flow. We found decreased expression of muscle atrophy-related genes in ischemic muscle, confirming the hypothesis that KD induces muscle atrophy by directly affecting muscle atrophy regulatory genes.

Reduced wound healing by calorie-restricted diet has been reported previously [29]; therefore, we observed wound healing after hind limb ischemia and found that KD delayed wound healing, increased toe necrosis rate, and increased severe inflammation at wound sites. We found that inflammation-related genes were significantly decreased in their ischemic limb tissues, indicating that reduced gene expression may be a reason for KD-induced inflammation. This was supported by previous studies showing that KD reduces inflammasome (NLRP3) and downregulates inflammation-related genes [24].

Another study reported that KD induced cardiac fibrosis in mice [30]; therefore, we evaluated fibrosis of ischemic limb tissue by Masson staining, and found that KD accelerated fibrosis in limb tissue after ischemia. We then found an increased gene expression of *Col2* and α -SMA followed by an elevated α -SMA protein level, with a further indication of fibrosis induced by KD.

Finally, we studied the metabolic status before and after ischemia by examining the gene and protein expression of metabolic enzymes and transporters. We found that KD significantly decreased glucose uptake by downregulating glucose transporter (GLUT1 and GLUT4) expression at the both gene and protein levels in hind limb tissue, and this was further aggregated by ischemia. The same was found for HK2, while PDK1 was upregulated by KD at both the gene and protein levels, indicating that KD also decreases glycolysis in limb tissue. We also examined CD36 and CPT1 expression, and found that KD increased fatty acid uptake in limb tissue before ischemia but decreased its uptake after ischemia, indicating that ischemia interferes with the effect of KD on fatty acid uptake by limb tissue. Decreased ketolysis in muscle tissue in KD mice has been reported [25], thus we evaluated the effect of KD on ketone metabolism in limb tissue before and after ischemia, and found that KD decreased ketolysis but did not affect ketogenesis of limb tissue before ischemia, while it further decreased ketolysis and increased ketogenesis after ischemia of limb tissue, indicating that ischemia accelerates KD's impact on ketone metabolism.

We reported impaired blood flow recovery after hind limb ischemia in mice, along with delayed wound healing and aggravated inflammation under KD, and found that KD induced muscle atrophy and accelerated fibrosis after ischemia; however, we did not further investigate the underlying mechanism of these findings; therefore, further studies are needed to clarify the possible mechanism induced by KD. We found that KD altered the metabolic status of limb tissue with or without ischemic conditions, but we did not further investigate the relation of metabolic alteration of limb tissue caused by KD with subsequent reduced angiogenesis, muscle atrophy as well as fibrosis. The underlying mechanism of metabolic alterations caused by KD and its effects on cellular function needs to be further studied.

Declarations

Funding

This work was supported by funding from the Innovative Research Groups of the National Natural Science Foundation of China (81521001), Major Research Plan of the National Natural Science Foundation of China (91639104), a grant to AS from the Innovation Program of Shanghai Municipal Education Commission, the National Science Fund for Distinguished Young Scholars (81725002).

Conflict of Interests

The authors have no relevant financial or non-financial interests to disclose.

Data availability: The data sets generated during and/or analyzed during the current 7 study are available from the corresponding author on reasonable request.

Author Contributions

Adilan Shalamu, Junbo Ge and AiJun Sun conceived and designed the study. Adilan Shalamu, Zhen Dong, Bowen Liu, Lihong Pan, Yun Cai and Liwei Liu performed the animal and cell culture experiments. Adilan Shalamu, Xiurui Ma, Kai Hu and Junbo Ge interpreted the data. Adilan Shalamu, Junbo Ge and Aijun Sun wrote the manuscript. Junbo Ge and Aijun Sun supervised the study. Junbo G and Aijun Sun reviewed and edited the manuscript. All authors approved the final manuscript.

Ethics approval

All animal experimental procedures conformed to the Guide for the Care and Use of Laboratory Animals published by the US National Institutes of Health (NIH publication no. 85–23, revised 1996) and were reviewed and approved by the Animal Ethics Committee at Zhongshan Hospital, Fudan University, China.

Consent to participate

References

1. Dhamija R, Eckert S, Wirrell E. Ketogenic diet. *Can J Neurol Sci.* 2013;40:158 – 67. doi: 10.1017/s0317167100013676. PMID: 23419562.
2. Wheless JW. History of the ketogenic diet. *Epilepsia.* 2008;49 Suppl 8:3–5. doi: 10.1111/j.1528-1167.2008.01821.x. PMID: 19049574.
3. Cahill GF Jr. Fuel metabolism in starvation. *Annu Rev Nutr.* 2006;26:1–22. doi: 10.1146/annurev.nutr.26.061505.111258. PMID: 16848698.
4. Johnson RH, Walton JL, Krebs HA, Williamson DH. Post-exercise ketosis. *Lancet.* 1969;2:1383-5. doi: 10.1016/s0140-6736(69)90931-3. PMID: 4188274.
5. Koeslag JH, Noakes TD, Sloan AW. Post-exercise ketosis. *J Physiol.* 1980;301:79–90. doi: 10.1113/jphysiol.1980.sp013190. PMID: 6997456; PMCID: PMC1279383.

6. Bolla AM, Caretto A, Laurenzi A, Scavini M, Piemonti L. Low-carb and ketogenic diets in type 1 and type 2 diabetes. *Nutrients*. 2019;11:962. doi: 10.3390/nu11050962. PMID: 31035514; PMCID: PMC6566854.
7. Walsh JJ, Myette-Côté É, Neudorf H, Little JP. Potential therapeutic effects of exogenous ketone supplementation for type 2 diabetes: a review. *Curr Pharm Des*. 2020;26:958 – 69. doi: 10.2174/1381612826666200203120540. PMID: 32013822.
8. Shukla SK, Gebregiworgis T, Purohit V, et al. Metabolic reprogramming induced by ketone bodies diminishes pancreatic cancer cachexia. *Cancer Metab*. 2014 Sep;2:18. doi: 10.1186/2049-3002-2-18. Erratum in: *Cancer Metab*. 2014;2:22. PMID: 25228990; PMCID: PMC4165433.
9. Poff AM, Ari C, Arnold P, Seyfried TN, D'Agostino DP. Ketone supplementation decreases tumor cell viability and prolongs survival of mice with metastatic cancer. *Int J Cancer*. 2014 Oct;135(7):1711–20. doi: 10.1002/ijc.28809. Epub 2014. PMID: 24615175; PMCID: PMC4235292.
10. De Feyter HM, Behar KL, Rao JU, et al. A ketogenic diet increases transport and oxidation of ketone bodies in RG2 and 9L gliomas without affecting tumor growth. *Neuro Oncol*. 2016;18:1079–87. doi: 10.1093/neuonc/nov088. Epub 2016 May 3. PMID: 27142056; PMCID: PMC4933488.
11. Goedeke L, Bates J, Vatner DF, et al. Acetyl-CoA carboxylase inhibition reverses NAFLD and hepatic insulin resistance but promotes hypertriglyceridemia in rodents. *Hepatology*. 2018;68:2197–211. doi: 10.1002/hep.30097. PMID: 29790582; PMCID: PMC6251774.
12. Rahman M, Muhammad S, Khan MA, et al. The β -hydroxybutyrate receptor HCA2 activates a neuroprotective subset of macrophages. *Nat Commun*. 2014;5:3944. doi: 10.1038/ncomms4944. PMID: 24845831.
13. Al-Zaid NS, Dashti HM, Mathew TC, Juggi JS. Low carbohydrate ketogenic diet enhances cardiac tolerance to global ischaemia. *Acta Cardiol*. 2007;62:381-9. doi: 10.2143/AC.62.4.2022282. PMID: 17824299.
14. Fitchett D, Zinman B, Wanner C, et al. Heart failure outcomes with empagliflozin in patients with type 2 diabetes at high cardiovascular risk: results of the EMPA-REG OUTCOME® trial. *Eur Heart J*. 2016;37:1526-34. doi: 10.1093/eurheartj/ehv728. Epub 2016 Jan 26. Erratum for: *Eur Heart J*. 2016 May 14;37(19):1535-7. PMID: 26819227; PMCID: PMC4872285.
15. Prattichizzo F, De Nigris V, Micheloni S, La Sala L, Ceriello A. Increases in circulating levels of ketone bodies and cardiovascular protection with SGLT2 inhibitors: Is low-grade inflammation the neglected component? *Diabetes Obes Metab*. 2018;20:2515–22. doi: 10.1111/dom.13488. Epub 2018 Sep 6. PMID: 30073768.
16. Kim DH, Park MH, Ha S, et al. Anti-inflammatory action of β -hydroxybutyrate via modulation of PGC-1 α and FoxO1, mimicking calorie restriction. *Aging (Albany NY)*. 2019;11:1283–304. doi: 10.18632/aging.101838. PMID: 30811347; PMCID: PMC6402511.
17. Viggiano A, Meccariello R, Santoro A, et al. A Calorie-Restricted Ketogenic Diet Reduces Cerebral Cortex Vascularization in Prepubertal Rats. *Nutrients*. 2019;11:2681. doi: 10.3390/nu11112681. PMID: 31694345; PMCID: PMC6893715.

18. Mukherjee P, El-Abbadi MM, Kasperzyk JL, Raney MK, Seyfried TN. Dietary restriction reduces angiogenesis and growth in an orthotopic mouse brain tumour model. *Br J Cancer*. 2002;86:1615–21. doi: 10.1038/sj.bjc.6600298. PMID: 12085212; PMCID: PMC2746602.
19. Lin BQ, Zeng ZY, Yang SS, Zhuang CW. Dietary restriction suppresses tumor growth, reduces angiogenesis, and improves tumor microenvironment in human non-small-cell lung cancer xenografts. *Lung Cancer*. 2013;79:111–7. doi: 10.1016/j.lungcan.2012.11.001. Epub 2012 Nov 28. PMID: 23199512.
20. Xin B, Liu CL, Yang H, et al. Prolonged fasting improves endothelial progenitor cell-mediated ischemic angiogenesis in mice. *Cell Physiol Biochem*. 2016;40:693–706. doi: 10.1159/000452581. Epub 2016 Nov 30. PMID: 27898404.
21. García-Caballero M, Zecchin A, Souffreau J, et al. Role and therapeutic potential of dietary ketone bodies in lymph vessel growth. *Nat Metab*. 2019;1:666 – 75. doi: 10.1038/s42255-019-0087-y. Epub 2019 Jul 12. PMID: 32694649.
22. Menger MM, Nalbach L, Roma LP, et al. Erythropoietin exposure of isolated pancreatic islets accelerates their revascularization after transplantation. *Acta Diabetol*. 2021;58:1637–47. doi: 10.1007/s00592-021-01760-4. Epub 2021 Jul 12. PMID: 34254190; PMCID: PMC8542558.
23. Mammucari C, Milan G, Romanello V, et al. FoxO3 controls autophagy in skeletal muscle in vivo. *Cell Metab*. 2007;6:458 – 71. doi: 10.1016/j.cmet.2007.11.001. PMID: 18054315.
24. Youm YH, Nguyen KY, Grant RW, et al. The ketone metabolite β -hydroxybutyrate blocks NLRP3 inflammasome-mediated inflammatory disease. *Nat Med*. 2015;2:263–9. doi: 10.1038/nm.3804. Epub 2015 Feb 16. PMID: 25686106; PMCID: PMC4352123.
25. Shimizu K, Saito H, Sumi K, et al. Short-term and long-term ketogenic diet therapy and the addition of exercise have differential impacts on metabolic gene expression in the mouse energy-consuming organs heart and skeletal muscle. *Nutr Res*. 2018;60:77–86. doi: 10.1016/j.nutres.2018.09.004. Epub 2018 Sep 19. PMID: 30527262.
26. Lien EC, Westermarck AM, Zhang Y, et al. Low glycaemic diets alter lipid metabolism to influence tumour growth. *Nature*. 2021;599:302–7. doi: 10.1038/s41586-021-04049-2. Epub 2021 Oct 20. PMID: 34671163; PMCID: PMC8628459.
27. Greene AE, Todorova MT, McGowan R, Seyfried TN. Caloric restriction inhibits seizure susceptibility in epileptic EL mice by reducing blood glucose. *Epilepsia*. 2001;42:1371-8. doi: 10.1046/j.1528-1157.2001.17601.x. PMID: 11879337.
28. Nakao R, Abe T, Yamamoto S, Oishi K. Ketogenic diet induces skeletal muscle atrophy via reducing muscle protein synthesis and possibly activating proteolysis in mice. *Sci Rep*. 2019;9:19652. doi: 10.1038/s41598-019-56166-8. PMID: 31873138; PMCID: PMC6928149.
29. Hunt ND, Li GD, Zhu M, et al. Effect of calorie restriction and refeeding on skin wound healing in the rat. *Age (Dordr)*. 2012;34:1453-8. doi: 10.1007/s11357-011-9321-6. Epub 2011 Oct 27. Erratum in: *Age (Dordr)*. 2012 Dec;34(6):1563. Miller, Marshall [added]. PMID: 22037865; PMCID: PMC3528375.

30. Xu S, Tao H, Cao W, et al. Ketogenic diets inhibit mitochondrial biogenesis and induce cardiac fibrosis. *Signal Transduct Target Ther.* 2021;6:54. doi: 10.1038/s41392-020-00411-4. PMID: 33558457; PMCID: PMC7870678.

Tables

Table1. Ingredient Composition

	Ketogenic Diet	Control Diet
Ingredient	gm	gm
Casein	163.8	94.21
L-Cystine	2.46	1.41
Corn Starch	0.00	349.51
Maltodextrin	0.00	32.97
Sucrose	0.00	382.48
Cellulose	81.9	47.1
Soybean Oil	40.95	23.55
Butter	624.08	18.84
Miner Mix S10026B	81.9	47.10
Vitamin Mix, V10001C, 10x Vits	1.64	0.94
Choline Bitartrate	3.28	1.88
FD&C Red Dye #40	0.025	0
FD&C Yellow Dye #5	0.025	0.025
FD&C Blue Dye #1	0	0.025
Total	1000	1000

Table 2. Primers for qPCR

Gene	Forward	Reverse
PECAM1	ACGCTGGTGCTCTATGCAAG	TCAGTTGCTGCCCATTCATCA
VEGFA	GCACATAGAGAGAATGAGCTTCC	CTCCGCTCTGAACAAGGCT
FOXO3	CTGGGGGAACCTGTCCTATG	TCATTCTGAACGCGCATGAAG
Map1lc3a	GACCGCTGTAAGGAGGTGC	CTTGACCAACTCGCTCATGTTA
IL-1 β	GCAACTGTTCTGAACTCAACT	ATCTTTTGGGGTCCGTCAACT
IL-6	TAGTCCTTCCTACCCCAATTTCC	TTGGTCCTTAGCCACTCCTTC
IL-18	GTGAACCCAGACCAGACTG	CCTGGAACACGTTTCTGAAAGA
Col1a2	TCGTGCCTAGCAACATGCC	TTTGTGAGAATACTGAGCAGCAA
α SMA	CCCAGACATCAGGGAGTAATGG	TCTATCGGATACTTCAGCGTCA
GLUT4	GTGACTGGAACACTGGTCCTA	CCAGCCACGTTGCATTGTAG
GLUT1	CAGTTCGGCTATAACTGGTG	GCCCCGACAGAGAAGATG
HK2	TGATCGCCTGCTTATTCACGG	AACCGCCTAGAAATCTCCAGA
PDK1	GGACTTCGGGTCAGTGAATGC	TCCTGAGAAGATTGTCGGGGA
CD36	ATGGGCTGTGATCGGAACTG	GTCTTCCCAATAAGCATGTCTCC
CPT1	GCACACCAGGCAGTAGCTTT	CAGGAGTTGATTCCAGACAGGTA
HMGCS2	GAAGAGAGCGATGCAGGAAAC	GTCCACATATTGGGCTGGAAA
BDH1	ACAAGACACACGCTGTTGTTT	CTCTTCAAGCTGTCCAGTTCC
SCOT	CATAAGGGGTGTGTCTGCTACT	GCAAGGTTGCACCATTAGGAAT
Actb	GGCTGTATTCCCCTCCATCG	CCAGTTGGTAACAATGCCATGT

Figures

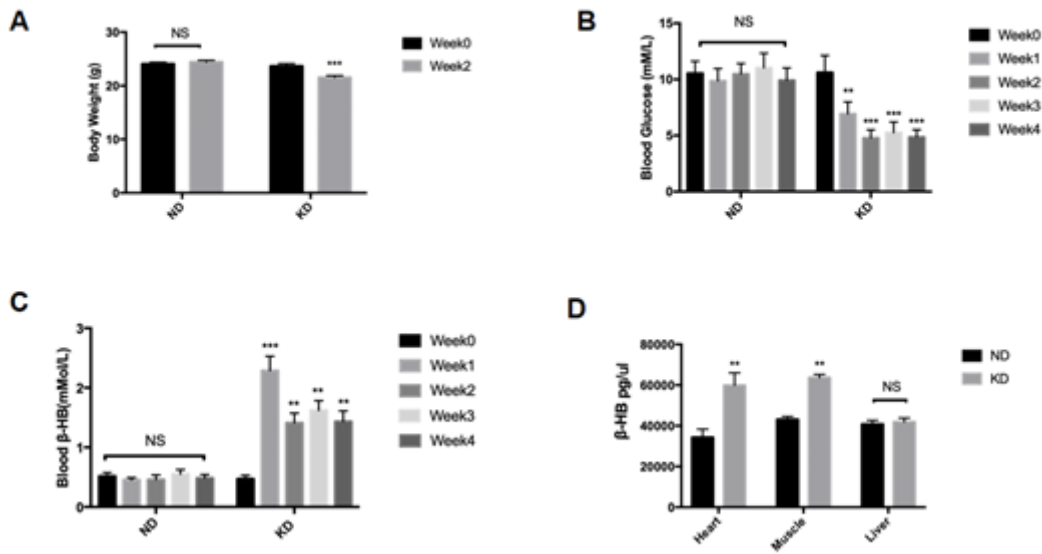


Figure 1

Body weight and blood metabolic parameters: **A** body weight changes of mice in the ND and KD groups during 2 weeks of feeding **B** observation of blood glucose levels during 4 weeks of feeding **C** observation of blood β -hydroxybutyrate level during 4 weeks of feeding **D** β -hydroxybutyrate concentration in heart, muscle and liver tissue. Mean \pm SEM, n=13, *P<0.05, **P<0.01, ***P<0.001.

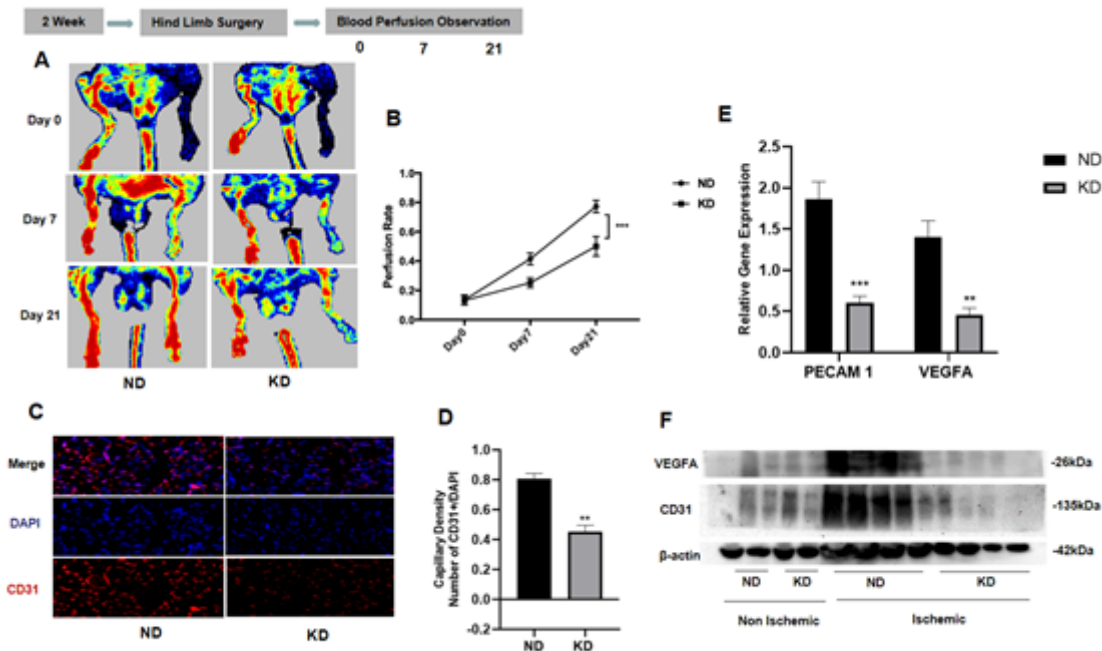


Figure 2

Effects of ketogenic diet on perfusion recovery, revascularization in chronic hindlimb ischemia; **A** original laser Doppler perfusion images displaying hindlimb perfusion 0, 7, and 21 days after excision of femoral artery; **B** perfusion recovery in ND and KD group mice at 7, and 21 days after surgery; **C** representative original micrographs of hindlimb sections 14 days after surgery, CD31 (+) stained are shown in green, DAPI-stained nuclei are shown in blue; **D** quantitative analysis of capillary density (Ratio of CD31 (+) cells and DAPI (+) cells); **E** relative gene expression of CD31 (PECAM) and VEGFA in ischemic hind limb 7 days after surgery; **F** protein expression of CD31 (PECAM) and VEGFA both in ischemic and non-ischemic limb 7 days after surgery. Mean±SEM, n=10 to 13, *P<0.05, **P<0.01, ***P<0.001.

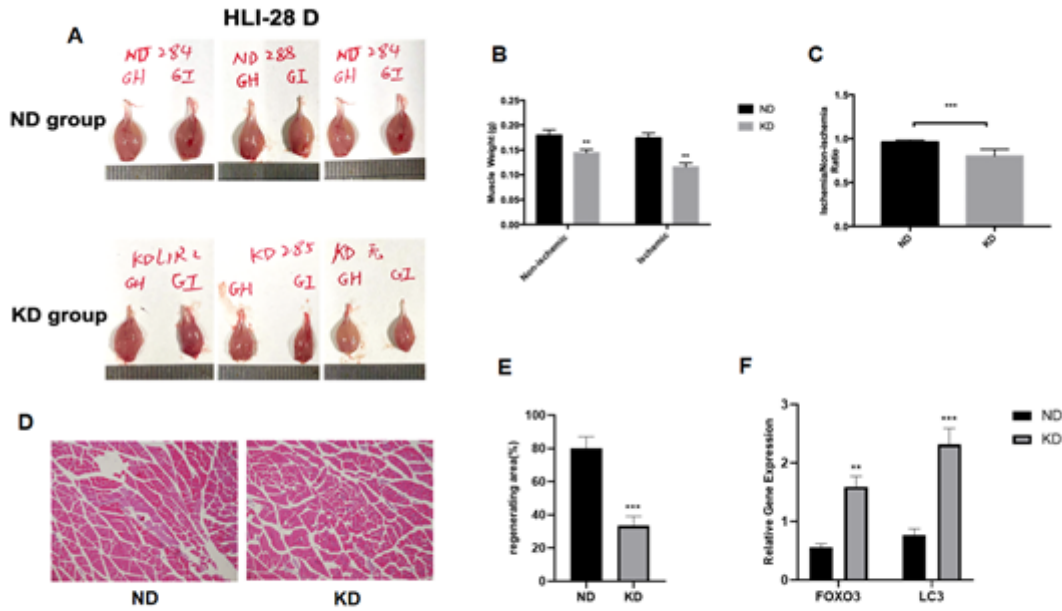


Figure 3

Quantitative analysis of gastrocnemius muscle atrophy. **A** images of ischemic limb and lateral limb muscle taken 28 days after surgery; **B** comparison of ischemic limb and lateral limb (non-ischemic) muscle weight between ND and KD groups, respectively; **C** comparison of ischemic limb/lateral limb muscle weight ratio between ND and KD groups; **D** representative hematoxylin-eosin staining images 28 days after hind limb surgery; **E** quantification of regenerating area, scale bar 10 mm; **F** relative gene expression of muscle atrophy related genes. Mean±SEM, n=10 to 13, *P<0.05, **P<0.01, ***P<0.001.

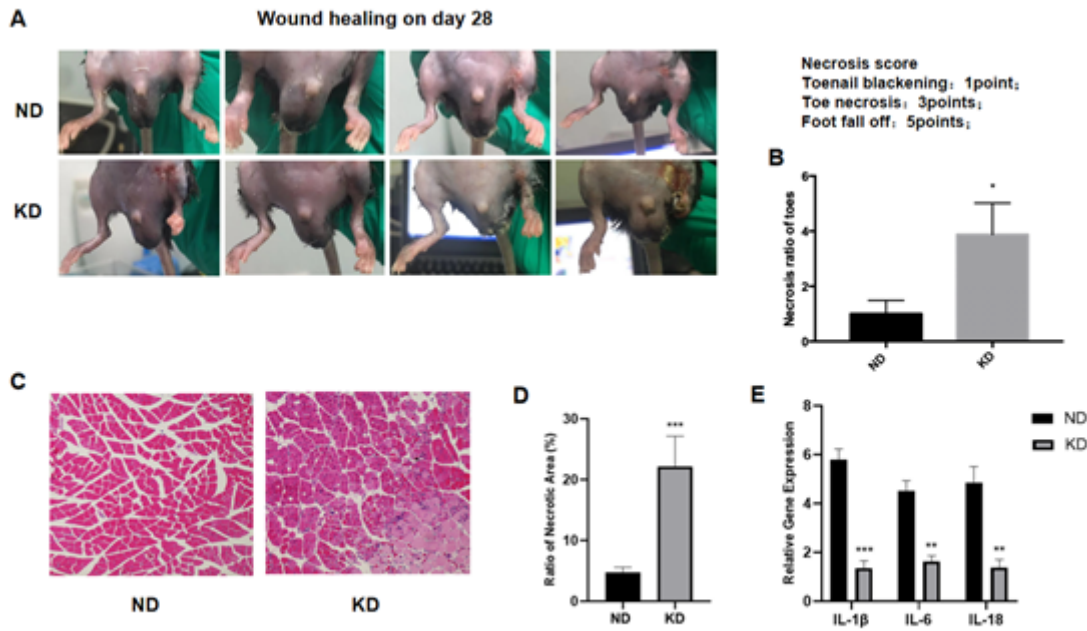


Figure 4

Effects of KD on wound healing in chronic hindlimb ischemia. **A** Image of surgical wounds 28 days after hind limb surgery; **B** comparison of necrosis ratio of toes between mice in the ND and KD groups; **C** representative hematoxylin-eosin (H&E) staining images 28 days after hind limb surgery; **D** comparison between ratio of necrotic area based on H&E staining in ND and KD group; **E** relative gene expression of inflammation related genes in ND and KD group respectively. Mean \pm SEM, n=8, *P<0.05, **P<0.01.

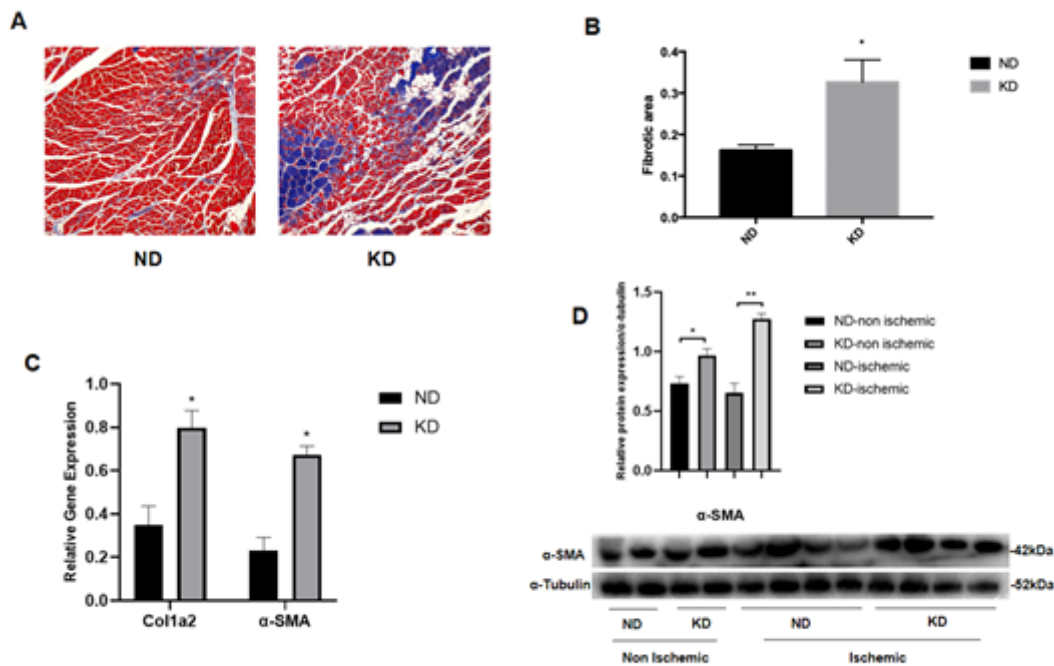


Figure 5

Effect of KD on fibrosis of hind limb tissue in chronic hindlimb ischemia. **A** Masson staining of ischemic limb tissue 28 days after hind limb surgery; **B** quantitative analysis of fibrotic area based on Masson staining; **C** relative gene expression of fibrosis related genes in ischemic tissues. **D** relative protein expression of α -SMA in both ischemic and non-ischemic tissues. Mean \pm SEM, n=8, *P<0.05.

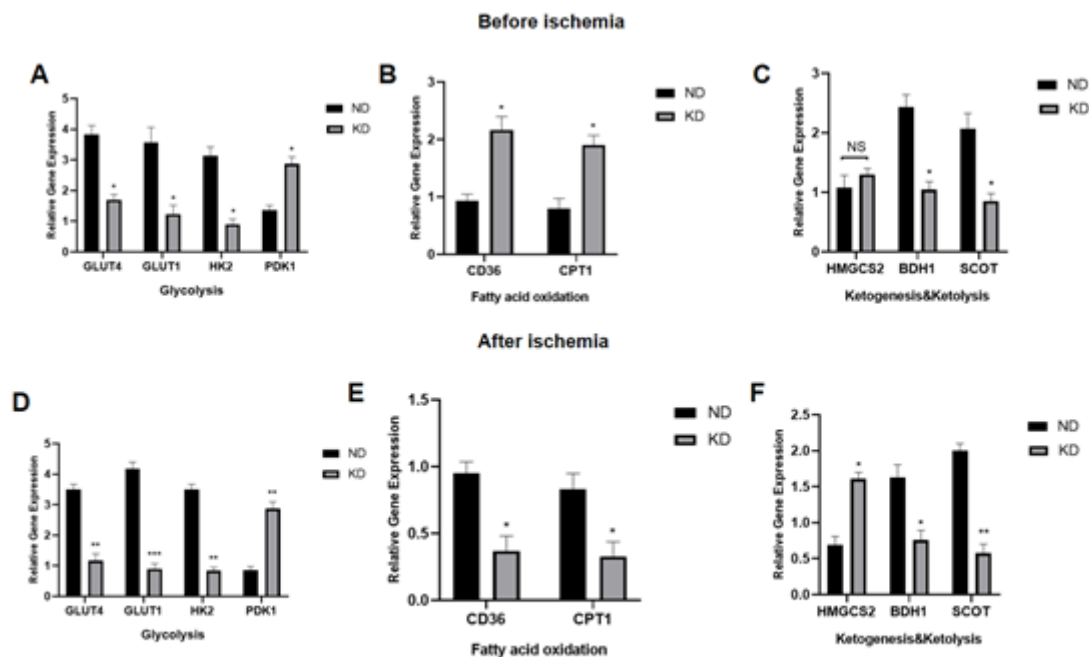


Figure 6

Metabolic changes in hind limb tissues at gene level before and after hind limb surgery. **A** Relative gene expression of glycolysis related genes in limb tissue before hind limb surgery; **B** relative gene expression of fatty acid oxidation related genes in limb tissue before hind limb surgery; **C** relative gene expression of ketone metabolism related genes in limb tissue before hind limb surgery; **D** relative gene expression of glycolysis related genes in limb tissue after hind limb surgery; **E** relative gene expression of fatty acid oxidation related genes in limb tissue after hind limb surgery; **F** relative gene expression of ketone metabolism related genes in limb tissue after hind limb surgery. Mean \pm SEM, n=8, *P<0.05, **P<0.01, ***P<0.001.

Figure 7

Metabolic change in hind limb tissues at protein level before and after hind limb surgery. **A** WB of hind limb tissue before and after hind limb surgery; **B** relative protein expression of GLUT4 in limb tissue before and after ischemic surgery and comparison between the two groups (ND and KD); **C** relative protein expression of GLUT1; **D** relative protein expression of HK2; **E** relative protein expression of PDK1; **F** relative protein expression of CPT1; **G** relative protein expression of BDH1; **H** relative protein expression of SCOT. Mean \pm SEM, n=8, *P<0.05, **P<0.01, ***P<0.001.